Journal of

Applied and Computational Mechanics

Shahid Chamran
University of Ahvaz

Research Paper

Multilevel Modeling of 1-3 Piezoelectric Energy Harvester Based on Porous Piezoceramics

Thanh Binh Do[1], Andrey Nasedkin[2], Pavel Oganesyan[2], Arcady Soloviev[1,2]

[1] Department of Theoretical and Applied Mechanics, Don State Technical University,
Gagarin sqr.1, Rostov on Don, 34400, Russia; Emails: dothanhbinh@mail.ru (T.B.D.), solovievarc@gmail.com (A.S.)

[2] Laboratory of Computational Mechanics, Institute of Mathematics, Mechanics and Computer Sciences, Southern Federal University,
Milchakova str. 8a, Rostov on Don, 344090, Russia; Emails: nasedkin@math.sfedu.ru (A.N.), oganesyan@hey.com (P.O.)

Abstract. The paper presents a computer analysis of the properties of a piezoelectric composite consisting of porous piezoceramic rods regularly arranged in an elastic matrix (piezocomposite with a connectivity of 1-3). The porous piezoceramic PZT-4 is used based on porous piezoceramics as an active material. The calculation of material properties is carried out based on a multilevel approach. First, the effective moduli of porous piezoceramics are determined, and then a 1-3 piezocomposite with rods having the calculated homogeneous properties is analyzed. The simulation uses the homogenization method based on the Hill lemma and the finite element method, as well as approximate analytical models. The effective properties of 1-3 composite are determined for various percentages of porosity of piezoceramic rods, which are a composite of 3-0 connectivity. Calculations were performed in the software package ACELAN-COMPOS. The calculated properties are used in finite element models to evaluate the effectiveness of composite materials in sensors and energy harvesting devices. Two cases of stiffness of an isotropic matrix are considered, which correspond to the stiffness of a porous composite at 50% and 80% porosity. The electromechanical properties, such as electro-mechanical coupling coefficient and output potential, for different transducers models made from the proposed composite are analyzed.

Keywords: Piezoelectric material; Porous piezoceramics; Composite; Energy harvesting; Homogenization; Modeling; Finite element method.

1. Introduction

The use of piezoelectric generators as elements of energy storage devices is becoming more and more widespread, including in wearable devices, vehicles, road surfaces. Piezo generators are classified as "green" energy sources that do not harm the environment during operation. The growing interest in research into piezoelectric materials for energy storage is evidenced by a large number of reviews published in recent years. In this way, we can note the review of reviews (!) in 2021 [1] and the reviews [2–8] not mentioned in [1], which appeared in 2021–2022. Multiple biomedical application for piezocomposites were presented in papers [9, 10]. The variety of applications includes medical equipment production, implants, on-body energy harvesting. For energy harvesting devices, the most used designs of piezoelectric generators are beam or plate elements, consisting of piezoelectric and elastic layers. Cymbal transducers and stack-type designs are also popular.

To increase the efficiency of piezoelectric transducers, research is being carried out to find the optimal configuration of the device: size, shape, electroplating and loading scheme, materials used. Nevertheless, despite many studies, the problems of determining efficient designs of piezoelectric generators and the problems of searching for piezomaterials with improved characteristics for energy storage devices remain very relevant. At the same time, the use of piezocomposite materials is one of the most promising areas for improving the quality of piezoelectric transducers. The most well-known and well-studied are fibrous piezocomposites or piezocomposites of 1-3 connectivity according to Newnham's terminology [11], containing rod piezoceramic elements in an elastic dielectric matrix.

Among the large number of works on 1–3 piezocomposites, we note, for example, analytical and computer investigations of the effective moduli presented in [12–19]. Other references can be found in the review [20]. Piezocomposites with 1-3 connectivity have high values of several characteristics important for applications: hydrostatic piezoelectric charge coefficient d_h, hydrostatic voltage coefficient g_h, thickness mode electromechanical coupling coefficient k_t, hydrostatic figure of merit (HFoM) $d_h g_h$, etc.

Macrofiber composites, originally developed for aviation industry, have also found their application into energy harvesting devices [21-24]. These miniature micropower generators are made in the form of thin beams and include piezoelectric fibers located in a dielectric medium. The fibers are placed in a single multilayer structure with interdigitated electrodes located on the

side surfaces of the beams on both sides. A comparative analysis of piezoelectric generators made of monolithic and composite piezoceramics, carried out in [23], showed a significant efficiency of using macrofiber composites.

To improve the characteristics of the 1-3 piezocomposite, it is possible to vary the materials of the piezoelectric fibers and the elastic dielectric matrix. Thus, porous materials can be used for the composite matrix, which have a lower Young's modulus and Poisson's ratio can change significantly [12, 24–28]. In [12], the approximations of the effective medium method were used, and in [27, 28], applying the approaches from [12], topological optimization of the porous structure of the matrix was carried out. In [25, 26], the Mori-Tanaka method was realized to determine the effective moduli, first for a porous matrix, and then it was also used to analyze 1–3 piezocomposites. In this case, in [25, 26], the location of pores relative to the direction of polarization was also varied, which, however, is difficult to implement in practice.

In [29], a 0-3 composite with piezoelectric particles in a porous matrix was simulated and it was noted that the use of a porous matrix does not improve the electromechanical properties of the 0-3 composite. However, the piezosensitivity coefficients were not analyzed in this study.

Another direction in the modification of composites is associated with the use of porous piezoceramics, which has recently come to be regarded as a promising active material for energy storage devices [2, 7, 8, 30–33]. Porous piezoceramics, in comparison with dense ones, have a lower acoustic impedance, higher piezosensitivity, and a number of high quality factors or figures of merit. Some studies have shown that the piezoelectric modulus d_{33} does not depend on the porosity for ceramics with a 3-0 connectivity (piezoelectric material with closed porosity), but with increasing porosity, the rigidity decreases. Thus, it is possible to obtain a higher output potential in piezoelectric energy harvesting elements that use this piezoelectric module. One of the types of such structures is a piezocomposite of 1-3 connectivity.

Present research, to some extent, combines approaches to the use of porous piezoceramics in piezoelectric fibers of the composite with 1-3 connectivity and to the variation of matrix materials with different stiffnesses. Namely, in this paper, the 1-3 piezoelectric composites are considered, in which porous piezoceramics is used as a piezoactive material. The aim of this work is to investigate the electromechanical properties of converters made of such a composite, in particular, the electromechanical coupling coefficient (EMCC) and the output potential, for various percentages of ceramic porosity and for various elastic stiffnesses of the matrix material. Since a complete model of a composite with pores is difficult for finite element analysis, the study is carried out based on a step-by-step calculation of the effective properties of composites: first for porous ceramics, then for a representative volume of a composite with a connectivity of 1-3. The paper presents a comparative analysis of the results of calculations to determine the effective properties of the composite and calculations based on the finite element method for a representative volume with 1-3 connectivity and an analytical approach. The effective material properties are then used for further calculations of the transducer models.

2. Computer and Mathematical Models

2.1 Computer Models of Composites

To calculate the effective properties of both porous piezoceramic material and 1-3 piezocomposite, we use the ACELAN-COMPOS finite element package, the capabilities of which are described in detail in [35, 36]. This package implements the solution of the homogenization problems described below in representative volumes with a wide range of input characteristics that allow us to control the internal structure of the composite. ACELAN-COMPOS is able to create cubic representational volumes composed of cubic finite elements for 3-0 connectivity composites, i.e. with a closed structure of inclusions, 3-3 composites, i.e. with an open structure of inclusions, and 1-3 composites. Examples of representative volumes of 3-3, 3-0 and 1-3 composites are shown in Fig. 1.

The 3-3 composite shown in Fig. 1(a) can be obtained by mixing two materials with different properties or can represent a material with high porosity. Along each phase of such composite, connected paths can be laid along any of the three coordinate directions. The 3-0 composite shown in Fig. 1(b) is a structure that can describe a body with inclusions or pores. The properties of such composites are dependent on the distribution of pores or inclusions. In some cases, the pores or inclusions are isolated and have a simple shape; in others they may intersect and form complex areas. However, in the 3-0 composite, the second phase cannot be traversed along the representative volume in any direction from start to finish. Figure 1(c) shows 1-3 composite. Combining elastic matrix with electro elastic rods allows to build both effective and reliable piezo transducers.

As noted above, a combination of 3-0 and 1-3 bond types of connectivity can be useful in terms of achieving efficient electromechanical properties. Therefore, here, as the active part of the transducer, we use 3-0 porous piezoceramic material that fills the rods in 1-3 composite. An isotropic elastic material is used as a matrix in the transducer.
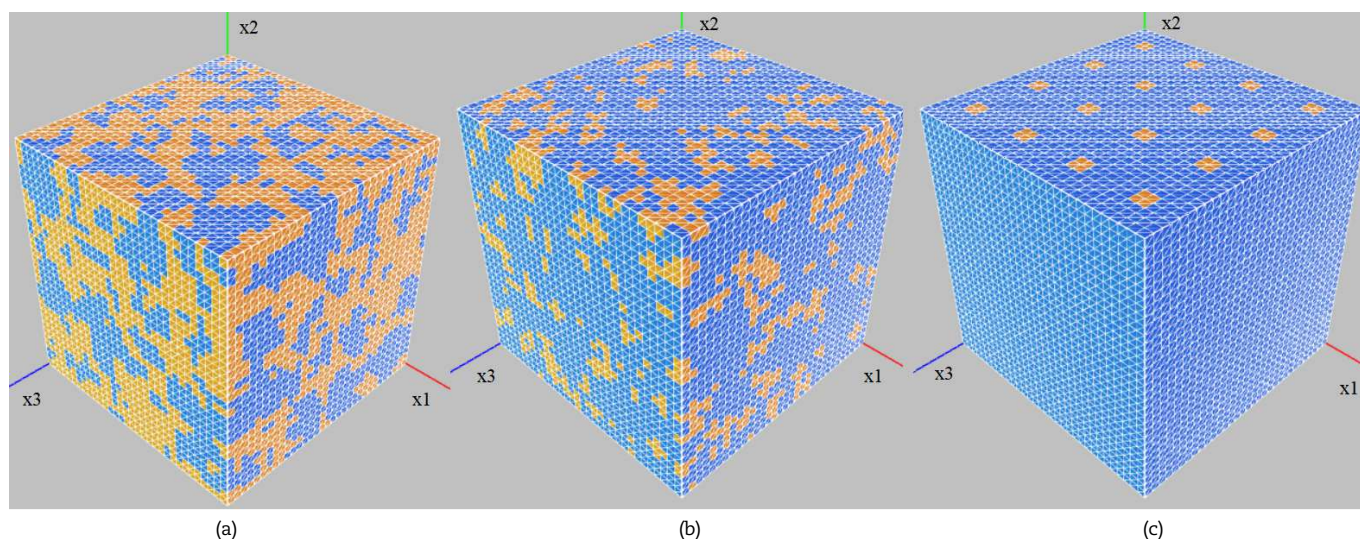

(a)   (b)   (c)

Fig. 1. Examples of Representative volumes of 3-3 (a), 3-0 (b) and 1-3 (c) composites.

2.2 Mathematical Model for Piezoelectric Bodies

For piezoelectric body V with heterogeneous material properties we will assume the following differential equation system [36, 37]

$$\sigma_{ij,j} + f_i = \rho \ddot{u}_i + \alpha_d \rho \dot{u}_i , \; D_{j,j} = 0 , \tag{1}$$

$$\sigma_{ij} = c_{ijkl}^E (\varepsilon_{kl} + \beta_d \dot{\varepsilon}_{kl}) - e_{kij} E_k , \qquad D_i + \varsigma_d \dot{D}_i = e_{ikl}(\varepsilon_{kl} + \varsigma_d \dot{\varepsilon}_{kl}) + \kappa_{ik}^S E_k , \tag{2}$$

$$\varepsilon_{kl} = (u_{k,l} + u_{l,k}) / 2 , \qquad E_k = -\varphi_{,k} , \tag{3}$$

where σ_{ij} and ε_{kl} are the components of the stress and strain tensors, D_i and E_k are the components of the electric induction and electric field vectors, u_i are the components of the displacement vector, φ is the scalar function of the electric potential, ρ is the density, f_i are the components of the mass force density vector, α_d, β_d, ς_d are the damping coefficients, c_{ijkl}^E are the components of the fourth order tensor of elastic stiffness moduli, evaluated at constant electric filed (E), e_{kij} are the components of the third order tensor of piezoelectric moduli, κ_{ik}^S are the components of the second order tensor of dielectric permittivities, evaluated at constant strains (S), which are often denoted by ε_{ik}^S. Here material constants can depend on spatial coordinates x_k, and the usual symmetry conditions are satisfied:, $c_{ijkl}^E = c_{jikl}^E = c_{klij}^E$, $e_{ikl} = e_{ilk}$, $\kappa_{ik}^S = \kappa_{ki}^S$.

Eqs. (1)–(3) differ from the usual equations of dynamic piezoelectricity by the presence of terms characterizing the attenuation (damping) properties. As noted in [36, 37], if $\varsigma_d = 0$ we obtain the equations of the theory of piezoelectricity with Rayleigh damping, which is like generally accepted in the finite element application. When the equality $\beta_d = \varsigma_d$ is satisfied, the system (1)–(3) is consistent with the mode superposition method. In the case of static problems, the damping is absent, and Eqs. (1)–(3) completely coincide with the standard equations of linear static piezoelectricity theory.

The system of differential equations (1)–(3) must also be supplemented with boundary conditions, and for transient problems it is also necessary to set the initial conditions. The boundary and initial conditions here do not differ from those usually accepted in the theory of piezoelectricity [35, 36].

2.3 Homogenization Technique and Computation of Effective Moduli

For piezoelectric composites, several formulations of homogenization problems are known destined to determine effective moduli. All these methods are a generalization of known approaches used for dielectric and elastic composite media. In the case of piezocomposites, these methods become much more complicated, due to the coupling of mechanical and electric fields caused by the piezoelectric effect, and the obligatory presence of anisotropy in the piezoelectric phase, which determines a large number of effective moduli to be defined. Among a significant number of investigations devoted to the homogenization problems for piezoelectric composite media, we note the papers [13, 14, 18, 19, 29, 30, 38-45], which describe various popular analytical, numerical-analytical, and numerical approaches.

However, since real porous piezomaterials have a complex irregular porosity structure, when formulating and solving the homogenization problem, it is preferable to consider the internal structure of the porous material, including the types of connectivity, pore sizes and scatter of their values, as well as various local effects. This can be done by constructing a representative volume element (RVE) of the appropriate type, and then solving the homogenization problem in this volume numerically using the finite element method. Then the formulation of the homogenization problem can be carried out by method of effective moduli [34, 35, 39, 43, 44]. We use this technique in the present study.

According to this method, we will solve the static problem of piezoelectricity in a RVE V with special essential boundary conditions on its boundary $\Gamma = \partial V$. For a static problem, all variables in the Eqs. (1)–(3) depend only on spatial coordinates x_k, and do not depend on time t. Therefore, Eqs. (1), (2) can be rewritten in the standard form

$$\sigma_{ij,j} = 0 , \qquad D_{j,j} = 0 , \tag{4}$$

$$\sigma_{ij} = c_{ijkl}^E \varepsilon_{kl} - e_{kij} E_k , \qquad D_i = e_{ikl} \varepsilon_{kl} + \kappa_{ik}^S E_k . \tag{5}$$

Boundary conditions in the effective moduli method should provide constant fields of strains, stresses, electric field, and electric induction for a homogeneous comparison medium. Usually, these boundary conditions are chosen to be linear on x_k for displacements and electric potential

$$u_l = x_k \varepsilon_{0kl} , \; \varphi = -x_k E_{0k} , \qquad x_k \in \Gamma , \tag{6}$$

where $\varepsilon_{0kl} = \varepsilon_{0kl}$ and E_{0k} are the components of the symmetric tensor of the second order and the vector, which are constant.

A homogeneous comparison medium has constant effective moduli effective moduli c_{ijkl}^{Eeff}, e_{ikl}^{eff}, κ_{ik}^{Seff}, and its constitutive relations between electromechanical fields, which we mark with the subscript "0", are similar to (5)

$$\sigma_{0ij} = c_{ijkl}^{Eeff} \varepsilon_{0kl} - e_{kij}^{eff} E_{0k} , \qquad D_{0i} = e_{ikl}^{eff} \varepsilon_{0kl} + \kappa_{ik}^{Seff} E_{0k} \tag{7}$$

Obviously, for a homogeneous medium, the functions $u_l = x_k \varepsilon_{0kl}$, $\varphi = -x_k E_{0k}$ are the solution to the boundary value problem (3)–(6) in RVE V with $c_{ijkl}^E = c_{ijkl}^{Eeff}$, $e_{ikl} = e_{ikl}^{eff}$, $\kappa_{ik}^S = \kappa_{ik}^{Seff}$ and determine the constant mechanical fields ε_{0kl}, σ_{0ij}, and the constant electric fields E_{0k}, D_{0i}, related by Eq. (7).

In addition, solutions of the boundary value problems (3)–(6) with inhomogeneous moduli c_{ijkl}^E, e_{kij}, κ_{ik}^S, and with effective moduli c_{ijkl}^{Eeff}, e_{ikl}^{eff}, κ_{ik}^{Seff}, are interconnected by important equalities [39, 43] $< \varepsilon_{kl} > = \varepsilon_{0kl}$, $< E_k > = E_{0k}$,

$$< \sigma_{kl} \varepsilon_{kl} > = < \sigma_{kl} > < \varepsilon_{kl} > = < \sigma_{kl} > \varepsilon_{0kl} , \qquad < D_i E_i > = < D_i > < E_i > = < D_i > E_{0i} , \tag{8}$$

where angle brackets mean volume averaging

$$< \bullet > = \frac{1}{|V|} \int_V (\bullet) \, dV . \tag{9}$$

By virtue of equalities (8), the composite medium and the homogeneous comparison medium under the same external influences (6) will have the identical average potential energies $<U> = U_0$, where $U = <\sigma_{kl}\varepsilon_{kl} + D_i E_i> / 2$, $U_0 = (\sigma_{0kl}\varepsilon_{0kl} + D_{0i}E_{0i}) / 2$, if the equalities $<\sigma_{ij}> = \sigma_{0ij}$, $<D_i> = D_{0i}$ are fulfilled.

The last two equalities underlie a convenient way to calculate the complete set of effective moduli based on solutions to the set of boundary value problems (3)–(6) with some nonzero components ε_{0kl} or E_{0k}.

In particular, we choose some fixed indices p, q (p, $q = 1, 2, 3$), and assume in the boundary conditions (6) the following values

$$\varepsilon_{0kl} = S_0(\delta_{kp}\delta_{lq} + \delta_{lp}\delta_{kq}) / 2, \qquad E_{0k} = 0, \tag{10}$$

where $S_0 = const$, δ_{kp} is the Kronecker symbol.

Then, after solving the boundary value problem (3)–(6), (10), it is necessary, using (9), to find the average stresses $\langle\sigma_{ij}\rangle$ and the average components of the electric induction vector $\langle D_j\rangle$, which determine the effective elastic stiffness moduli and effective piezoelectric moduli, respectively

$$c_{ijpq}^{Eeff} = \langle\sigma_{ij}\rangle / S_0, \qquad e_{jpq}^{eff} = \langle D_j\rangle / S_0. \tag{11}$$

Then, we choose some fixed index $p = 1, 2, 3$, and accept in the boundary conditions (6) such values ($E_0 = const$)

$$\varepsilon_{0kl} = 0, \qquad E_{0k} = E_0\delta_{kp}, \tag{12}$$

Now, the solutions of the problems (3)–(6), (12) allow us to find once again the effective piezoelectric moduli and the effective permittivities from the average stresses and from the average electric inductions

$$e_{pij}^{eff} = -\langle\sigma_{ij}\rangle / E_0, \qquad \kappa_{jp}^{Seff} = \langle D_j\rangle / E_0. \tag{13}$$

For a piezoelectric composite with an arbitrary class of physical anisotropy and/or for an irregular RVE with a pronounced geometric anisotropy, nine homogenization problems (3)–(6) must be solved to determine the full set of effective moduli: six problems (3)–(6), (10) with mechanical effects at $p = q = m$, $m = 1, 2, 3$; $p = 2$, $q = 3$; $p = 1$, $q = 3$; $p = 1$, $q = 2$; and three problems (3)–(6), (12) with electrical influences at $p = 1, 2, 3$. In this case, the effective stiffness moduli and dielectric moduli should have the same symmetry as the moduli of a conventional dense piezoelectric material, and the same type piezomoduli found from the solutions of the problems (3)–(6), (10) by (11) and from the solutions of the problems (3)–(6), (12) by (13) should be equal [44]. These statements are not entirely trivial, since the effective moduli are found from numerical solutions of different boundary value problems. Naturally, in the numerical solution of homogenization problems, the corresponding equalities are satisfied up to the computational errors.

Hereinafter, we will apply for material moduli the Voigt notations generally accepted in the theory of piezoelectricity. According to these notations, instead of tensors, we use the matrix of elastic stiffnesses $c_{\alpha\beta}^E$ of size $6x6$, the matrix of piezomoduli of size $3x6$, and the matrix of dielectric permittivity coefficients of size $3x3$. Then the following correspondence laws are adopted between the components of matrices and tensors: $i, j, k, l = 1, 2, 3$; $\alpha, \beta = 1, 2, ..., 6$; $c_{ijkl}^E = c_{\alpha\beta}^E$; $e_{ikl} = e_{i\beta}$; $(ij) \leftrightarrow \alpha$, $(kl) \leftrightarrow \beta$, $(11) \leftrightarrow 1$, $(22) \leftrightarrow 2$, $(33) \leftrightarrow 3$, $(23) \sim (32) \leftrightarrow 4$, $(13) \sim (31) \leftrightarrow 5$, $(12) \sim (21) \leftrightarrow 6$.

Note that piezoceramic materials that are used in industrial applications have an anisotropy class $6mm$, and their moduli matrices have the form

$$\mathbf{c}^E = \begin{bmatrix} c_{11}^E & c_{12}^E & c_{13}^E & 0 & 0 & 0 \\ & c_{11}^E & c_{13}^E & 0 & 0 & 0 \\ & & c_{33}^E & 0 & 0 & 0 \\ & & & c_{44}^E & 0 & 0 \\ & sym & & & c_{44}^E & 0 \\ & & & & & c_{66}^E \end{bmatrix}, \quad \mathbf{e} = \begin{bmatrix} 0 & 0 & 0 & 0 & e_{15} & 0 \\ 0 & 0 & 0 & e_{15} & 0 & 0 \\ e_{31} & e_{31} & e_{33} & 0 & 0 & 0 \end{bmatrix}, \quad \mathbf{k}^S = \begin{bmatrix} \kappa_{11}^S & 0 & 0 \\ 0 & \kappa_{11}^S & 0 \\ 0 & 0 & \kappa_{33}^S \end{bmatrix}, \tag{14}$$

and $c_{66}^E = (c_{11}^E - c_{12}^E) / 2$.

Then, if the RVE does not have a pronounced anisotropy, then the matrices of effective moduli of porous piezoceramics also have the structure (14). During calculations, we verified that the homogeneous piezoceramic had the same anisotropy class.

The described homogenization method maintains the energy balance between the composite and a homogeneous comparison medium based on the Hill lemma and is valid for piezoelectric composites of any connection with conditions of full contact between materials of different phases, and also for composites with extreme phase properties [44, 46]. If there are imperfections on the interface, it is necessary to modify this method to take into account the integral values on the interface boundary [47].

The solution of these problems in representative volumes of a complicated structure is possible only numerically, and the finite element method is usually used for this purpose. We used the ACELAN-COMPOS package, whose finite element technologies are described in detail in [34, 35]. The ACELAN-COMPOS package has variety algorithms for generation composite structures of 3-0, 3-3, and 1-3 connectivity that support many input parameters of representative volume elements. In the present study, it was used to calculate 3-0 and 1-3 piezocomposites.

3. Results and Discussion

3.1 Numerical Results for 3-0 Composite

ACELAN-COMPOS supports two main inclusion distribution algorithms for 3-3 and 3-0 composites.

In the 3-3 composite, both phases are three-dimensionally connected, and each phase can be passed through from the beginning to the end of the representative volume element (RVE) in three spatial directions. For an algorithm that generates a 3-3 composite, one component, which we will call Phase 1, is initially structurally interconnected, and all inclusions are contained in Phase 2. The process of modeling the composite starts with splitting the RVE into equal clusters. In each cluster the set of finite elements is selected on the surface. The sets for neighbor clusters are built with the respect for connectivity. The size of each

cluster is limited to 512 or 2048 elements, but the whole RVE can have much more elements. Splitting RVE into clusters allows to perform the algorithm of material distribution in parallel. The connectivity of the Phase 2 is checked on every step before adding next element to Phase 1. Only elements that can be excluded from Phase 2 without breaking its connectivity are considered as candidates for Phase 1. Setting the surface elements to connect clusters limits the minimum percentage of Phase 1 material to 15% but reverting the algorithm by swapping labels for Phase 1 and Phase 2 allows to set the limit of 5-95% for each phase.

In case of modeling 3-0 composites, percent of inclusion is not the only parameter to consider. There are multiple possible inclusion distributions, depending on the manufacturing process. Inclusions can have similar size or may be vary from small to large. The surface of the RVE may have inclusions or not. In some cases, inclusions can intersect and form larger structures with unpredictable shape. We consider both solid-solid 3-0 composites and solid-air porous composites, both types can be constructed in ACELAN-COMPOS package. For such composites connectivity is guaranteed only for Phase 1, and Phase 2 may be interconnected or not, depending on the inclusion percentage.

This approach was used in our previous works [48, 49] and [30] which was focused on electromechanical properties of 3-0 composite presented on Fig. 2.

When modeling porous ceramics, cavities arising in the composite were simulated as a pseudo-material with the dielectric constant of air and artificial elastic properties 10 orders of magnitude smaller than that of ceramics. This approach makes it possible to use a unified process for assembling the global stiffness matrix of the problem.

Numerical results for 3-0 composite made with PZT-4 are presented in Table 1 [30].

Here, in the calculation, we assumed that the pores are located randomly in the composite, are isolated, and slightly differ in volume from each other. Since porous piezoceramics are created artificially using pore formers, the pore sizes and total porosity are quite controllable parameters. To model such a composite, we used the 3-0 algorithm of the ACELAN-COMPOS package with representative volumes containing 2^n finite elements along each axis with $n = 5$. The pore sizes varied from 4 to 8 finite elements, but the algorithm allowed the pores to stick together within the domain (regular region containing $8^3 = 512$ finite elements). An example of such a representative volume is shown in Fig. 2 on the left. The accuracy of the results was checked as follows. Since the 3-0 algorithm of the ACELAN-COMPOS package generates a volume with a partially random porosity structure, the calculations were carried out several times, the relative error was determined, and the average values were calculated. The size of the representative volume was determined by a compromise between the speed of calculations and the stabilization of results in calculations with different n. Such an approach, as is known [50-52], makes it possible to simulate composites with a random structure that has some controllable parameters. More complex algorithms with an irregular mesh of finite elements [51-53] were not used here, since if applied to piezoelectric composites, the calculations would be too expensive, but the spread of the initial values of material properties and data on the internal structure does not require high accuracy in calculating the effective moduli.
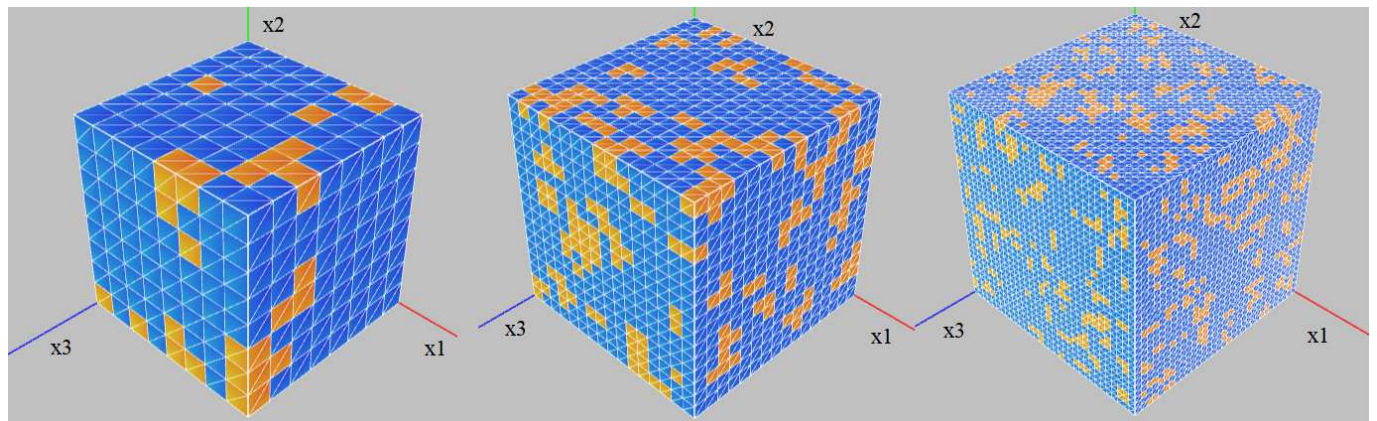

Fig. 2. Representative volumes for 3-0 composite generated in ACELAN-COMPOS package.

Table 1. Effective moduli of porous ceramics.

| % of porosity	0	10	20	30	40	50	60	70	80
ρ, 10^3, kg/m^3	7.5	6.75	6	5.25	4.5	3.75	3	2.25	1.5
$c_{11}^{E\,eff}$, GPa	139	115.6	92.5	68.5	50.5	33.4	20.7	12.6	6.8
$c_{12}^{E\,eff}$, GPa	77.8	61.5	46.6	31.4	21.0	11.6	6.2	2.8	1.3
$c_{13}^{E\,eff}$, GPa	74.3	58.2	42.5	28.2	18.7	10.6	5.2	2.4	1
$c_{33}^{E\,eff}$, GPa	115	95.3	72.3	54.2	39.1	27.2	16.3	9.1	4.7
$c_{44}^{E\,eff}$, GPa	25.6	22.3	18.3	14.4	11	7.4	4.4	2.3	1
e_{31}^{eff}, C/m^2	-5.2	-4.23	-3.14	-2.07	-1.32	-0.75	-0.43	-0.21	-0.1
e_{33}^{eff}, C/m^2	15.1	13.38	11.37	9.59	7.68	5.93	3.93	2.30	1.25
e_{15}^{eff}, C/m^2	12.7	10.96	8.96	6.91	5.00	3.30	1.95	1.00	0.44
$\kappa_{11}^{S\,eff}/\varepsilon_0$	730	663	582	509	439	349	263	191	122
$\kappa_{33}^{S\,eff}/\varepsilon_0$	635	567	492	413	345	270	199	130	75

Table 2. Effective moduli of 1-3 composite with matrix 1.

% of porosity	0	10	20	30	40	50	60	70	80
ρ , 10^3, kg/m^3	5.25	5.05	4.88	4.69	4.5	43.1	41.3	39.4	3.75
$c_{11}^{E\,eff}$, GPa	63.6	61.2	58.3	54.4	50.5	45.4	40.5	36.3	32.7
$c_{12}^{E\,eff}$, GPa	27.7	26.6	25.2	23.1	20.9	18	15.3	12.8	10.9
$c_{13}^{E\,eff}$, GPa	28.2	26.7	24.8	22.5	20.3	17.8	15.4	13.6	12.2
$c_{33}^{E\,eff}$, GPa	62.2	58.9	55.1	51.2	47.6	44.3	40.8	38.3	36.7
$c_{44}^{E\,eff}$, GPa	16.4	15.8	15.1	14.3	13.5	12.5	11.6	10.8	10.2
e_{31}^{eff} , C/m^2	-1.3	-1.05	-0.785	-0.523	-0.33	-0.185	-0.108	-0.053	-0.025
e_{33}^{eff} , C/m^2	3.77	3.35	2.86	2.4	1.93	1.49	0.972	0.58	0.32
e_{15}^{eff} , C/m^2	3.66	3.26	2.81	2.31	1.83	1.3	0.845	0.465	0.221
$\kappa_{11}^{S\,eff} / \varepsilon_0$	51.4	46.5	40.7	35.2	30.1	24.1	18.3	13.1	8.61
$\kappa_{33}^{S\,eff} / \varepsilon_0$	159	142	124	104	86.9	68.2	50.5	33.2	19.5

Table 3. Effective moduli of 1-3 composite with matrix 2.

% of porosity	0	10	20	30	40	50	60	70	80
ρ , 10^3, kg/m^3	3	2.81	2.63	2.44	2.25	2.06	1.88	1.69	1.5
$c_{11}^{E\,eff}$, GPa	11.50	11.30	11.00	10.60	10.20	9.56	8.82	7.96	6.85
$c_{12}^{E\,eff}$, GPa	2.37	2.33	2.28	2.22	2.14	2.02	1.86	1.58	1.33
$c_{13}^{E\,eff}$, GPa	3.32	3.15	2.94	2.69	2.46	2.19	1.84	1.55	1.25
$c_{33}^{E\,eff}$, GPa	22.50	20.30	17.80	15.40	13.20	11.20	9.04	7.40	6.32
$c_{44}^{E\,eff}$, GPa	4.25	4.15	4.03	3.88	3.69	3.41	3.04	2.61	2.19
e_{31}^{eff} , C/m^2	-1.30	-1.05	-0.79	-0.52	-0.33	-0.19	-0.11	-0.05	-0.03
e_{33}^{eff} , C/m^2	3.77	3.35	2.86	2.39	1.93	1.49	0.97	0.58	0.31
e_{15}^{eff} , C/m^2	1.44	1.35	1.24	1.10	0.96	0.78	0.59	0.38	0.21
$\kappa_{11}^{S\,eff} / \varepsilon_0$	14.1	12.9	11.5	10.1	8.9	7.39	5.93	4.62	3.47
$\kappa_{33}^{S\,eff} / \varepsilon_0$	159	142	123	104	86.9	68.2	50.5	33.2	19.5

The studies carried out have shown that for a certain configuration of the transducer, ceramics with a porosity of 40% demonstrate the highest EMCC [30]; however, in the general case, it is required to analyze each individual configuration of the transducer. In addition, the decrease in the strength of porous ceramic devices must be considered. As can be seen from Table 1, elastic moduli decrease with increasing porosity much faster than piezomoduli. As was noted in [30, 43], the piezomodulus d_{33}^{eff} remains the almost unchanged with the increase of porosity.
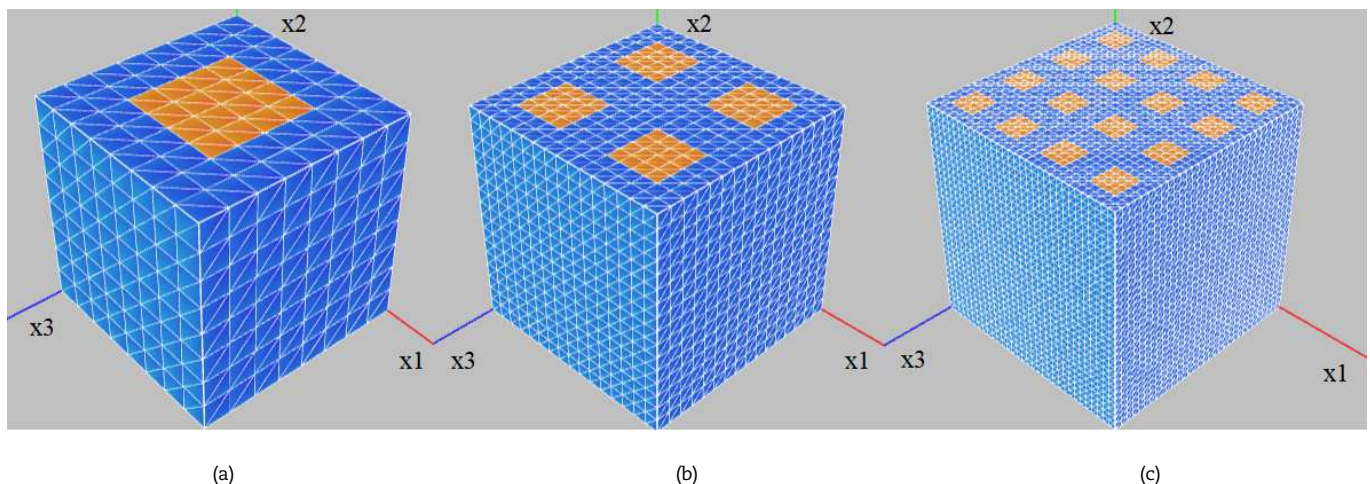
Fig. 3. Representative volumes for 3-0 composite generated in ACELAN-COMPOS package.

3.2 Numerical Experiments for 1-3 Composite

In this paper we study a composite with the geometry shown in Fig. 3. Piezoelectric rods with a square cross section are oriented along the Oz axis in an isotropic polymer matrix. The volume fraction of piezoelectric ceramics in the composite is 25%. In the course of numerical experiments, three representative volume elements were considered for the same material: with 1, with 4, and with 16 rods (Fig. 3(a), Fig. 3(b), Fig. 3(c), respectively). In addition to the number of rods in the investigated representative volumes, the size of the finite element changed. The problem of identifying the properties of a material with a representative volume in the form of a cube by the configuration shown in Figure 1 makes it possible to use a regular finite element mesh. In such a mesh, all elements have the same size and location in space with an accuracy of parallel transfer and differ only in the type of material. In this case, you can use caching of local stiffness matrices, calculating them only once for each material. Homogenization was performed for each representative volume and the difference in results was below 3%. Results obtained with model shown in Fig. 3(c) were used in this study, but it worth noting that even rough meshes can be sufficient for some composite types with regular structure.

When analyzing 1-3 composite, all options for the material of the rods from Table 1 were considered, the material of the matrix was presented in two versions, corresponding in stiffness in Ox_3 direction and density to ceramics with a porosity of 50% (hereinafter referred to as matrix 1) and 80% (matrix 2). Matrix 1 had Young's modulus equal to 27.2 GPa, matrix 2 – 4.7 GPa, Poisson's coefficient was equal to 0.3 for both matrices. These Young's moduli were chosen to match the stiffness of piezo material with porosity 50% and 80% in the direction of x_3 axis. The selection of these values is based on the fact that 80% is the largest percentage of porosity that effective materials properties were obtained on the first step of this research. But since 80% pores in practice can lead to rather fragile structure, moderate porosity of 50% was also chosen.

For most types of composites, the formation of a finer finite element mesh allows a more accurate solution to be obtained. So, in the case of 3-0 composite, the approximation of pores by spatial polygons consisting of cubes of the same size becomes more accurate as the size of finite elements decreases and their number increases. But for 1-3 composite, no significant difference was found between the simplest 512-element model and the 32768-element model. A significant role here is played by the simple shape of the common boundary between the two phases of the composite, on which excessive stresses, typical for models of composite materials with 3-0 connectivity, do not arise. At the same time, for the basic model with the simplest grid, solving a series of averaging problems in the ACELAN-COMPOS complex for 9 versions of piezoceramics and two versions of the polymer (162 boundary value problems in total) in the parallelization mode of tasks on a modern household computer takes about 90 seconds, including post-processor processing and saving the results. Thus, it becomes possible to design iterative processes for selecting the configuration of the composite.

ACELAN-COMPOS package was used to calculate the effective properties for both variants of composite. Numerical experiments were performed for the model with 16 rods.

The results of calculating the effective moduli for two types of matrix materials by the averaging method for 1–3 composites are shown in Tables 2 and 3.
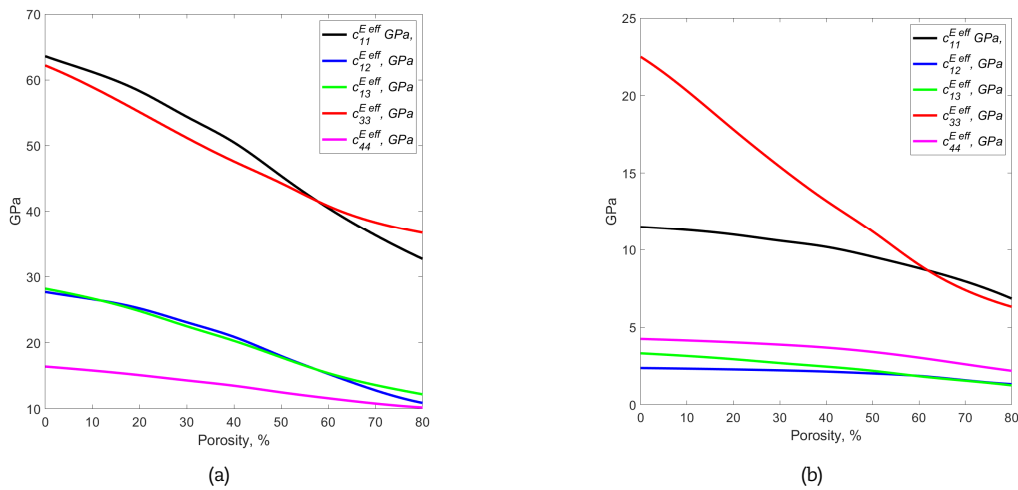

(a)   (b)

Fig. 4. The change in the elastic properties of the composite with an increase in the percentage of porosity of the piezoceramic for matrix 1 (a) and 2 (b).
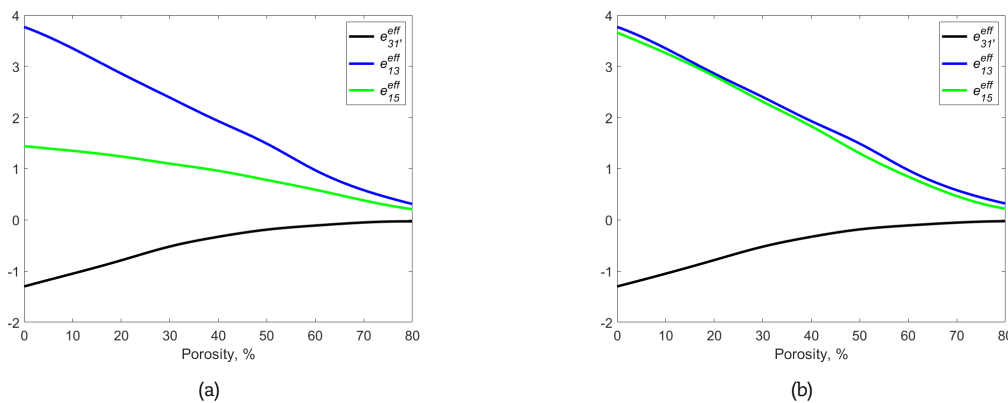

(a)   (b)

Fig. 5. Changes in the piezoelectric constants of the composite with an increase in the percentage of porosity of piezoceramics for matrix 1 (a) and matrix 2 (b).
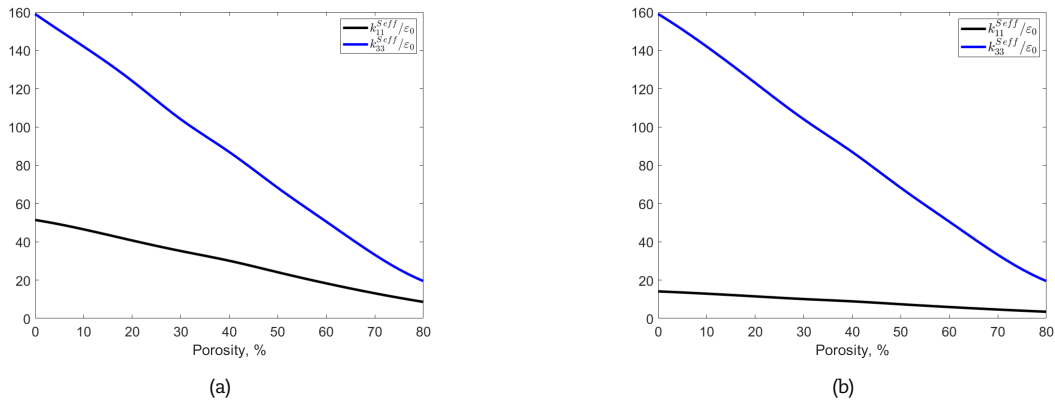
Fig. 6. Changes in the relative dielectric permittivity of the composite with an increase in the percentage of porosity of piezoceramics for matrix 1 (a) and matrix 2 (b).
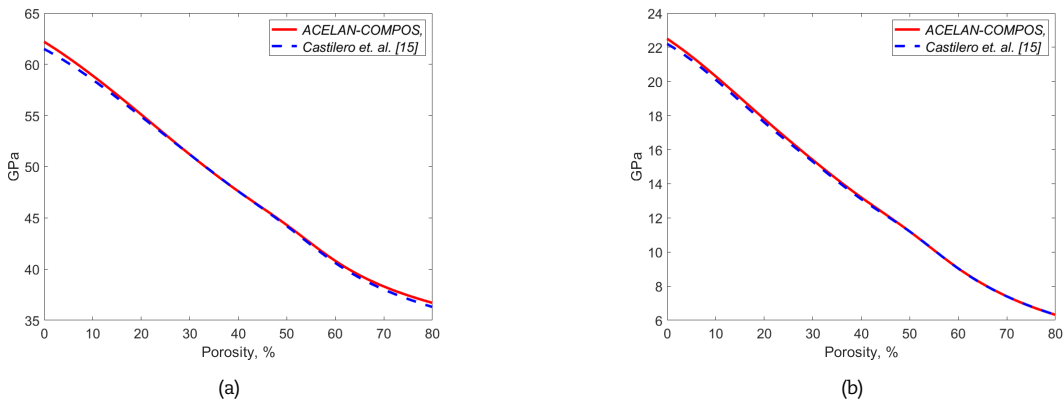

Fig. 7. Elastic stiffness modulus c_{33}^{Eeff} obtained on the basis of various approaches, for matrices 1 (a) and 2 (b).

For clarity, the results for mechanical properties, for electromechanical properties and for dielectric permittivities are also presented in Figs. 4, 5 and 6, respectively.

For composites with rod (fiber) inclusions, there are approximate asymptotic homogenization method for evaluating effective properties [15, 17]. In this study we focus on c_{33}^{Eeff} that can be approximated by the following equations:

$$c_{33}^{Eeff} = \left\langle c_{33}^{E} \right\rangle + \frac{\lambda \Delta_3^2 \alpha_1}{c_{66}^{Em}},$$

$$\langle * \rangle = (*)^m (1-\lambda) + (*)^f (\lambda), \qquad \Delta_3 = c_{13}^{Em} - c_{13}^{Ef},$$

$$\alpha_1 = \frac{(\chi^f - 1)(\lambda - 1)}{2\alpha_0}, \qquad \alpha_0 = \chi^*(1-\lambda) + (\chi^f - \lambda)\left(\frac{1}{2} + \frac{\lambda}{(\chi^m - 1)}\right),$$

$$\chi^j = 3 - 4\frac{c_{12}^{Ej}}{(c_{11}^{Ej} + c_{12}^{Ej})}, \quad j = f, m, \qquad \chi^* = \frac{c_{66}^{Ef}}{c_{66}^{Em}},$$

(15)

where m represents material properties of the matrix, f represents material properties of the rods or fibers, λ is the volume fraction of inclusion (fibers).

The calculation results based on the homogenization method in ACELAN-COMPOS and on the approximate formulas [15, 17] are shown in Fig. 7. The relative difference between ACELAN-COMPOS results and theoretical approximations does not exceed 2%.

At high porosity of piezoceramics, all methods show approximately the same values, however, at low porosity, the approximate method [15] gives less accurate results compared to the averaging method implemented in ACELAN-COMPOS.

3.3 Numerical Experiments for Transducer with Composite Material

The shape of a separate element of the transducer is shown in Fig. 8. The length of the transducer is 5 mm, the front is a square with 0.4 mm side. Both sides' frontal surfaces have electrodes. On one end, the boundary conditions of the sliding embedding are set, and the other end is free from stresses for modal analysis. This model was created in COMSOL Multiphysics [54] software.

Evaluation of efficiency was carried out based on two parameters: the EMCC and the output potential in the operating mode. To determine the EMCC, we used the following formula

$$k_{dj}^2 = \frac{f_{aj}^2 - f_{rj}^2}{f_{aj}^2},$$

(16)

where f_{rj} is the resonance frequency, f_{aj} is the antiresonance frequency, k_{dj} is the dynamic EMCC, and the subscript j denotes the number of resonance or antiresonance frequency.

To determine the resonance frequencies, eigenvalue problems with zero potentials on two electrodes were solved, and to determine the antiresonance frequencies, the boundary condition on one of the electrodes was changed to the free electrode condition.
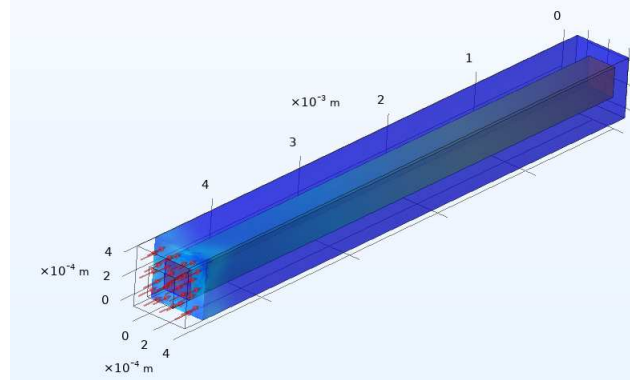
Fig. 8. Solid model of the transducer with internal square piezoelectric rod and with elastic isotropic filler.

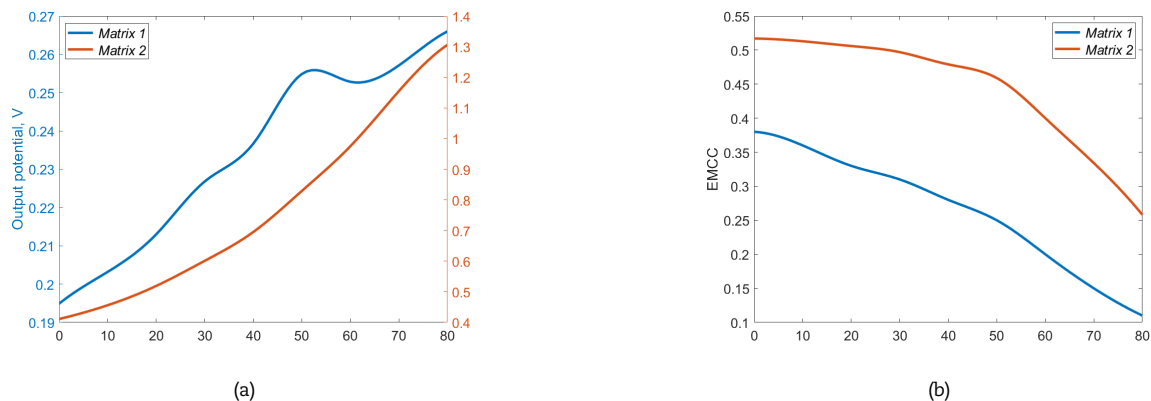(a)   (b)

Fig. 9. Dependence of the output potential (a) and of the EMCC (b) on the percentage of porosity of the ceramic.

Harmonic vibrations with a frequency of 1 kHz are considered as the operating mode of the transducer with one free electrode. This frequency is significantly lower than first eigenfrequency. The oscillations were created by applying distributed load with amplitude of 1000 N/m^2 at the loose side of the transducer. Red arrows in Fig. 8 demonstrate the pressure applied to the free side of the device. The problem was considered in two settings: in the form of a model of two solid bodies (a rod and an isotropic matrix) and in the form of a single piezoelectric body with effective material properties. The use of effective material properties makes it possible to simplify the process of finite element modeling, because the geometry of the model has no internal boundaries that increase the number of elements, and boundary conditions are set on a smaller number of surfaces. In the presented numerical experiments for one structural element, the two-solid model consisted of 2291 volumetric elements; with the same settings of the partition module, the model based on effective moduli consisted of 536 elements. As the geometry of the device becomes more complex, the difference in the number of elements will increase. In this case we used model with one rod presented on Fig. 8.

In the eigenvalue problem, the difference between the resonance frequency for the full compound model and for the model with effective properties does not exceed 0.5%, the difference in the output potential does not exceed 3%. All further numerical experiments were carried out for a model with effective properties. Figure 9(a) shows the dependence of the output potential under forced vibrations for all combinations of the porosity of the piezoceramics with the dense polymer matrix. In Fig. 9(b) shows a similar dependence for the EMCC at the first eigenfrequency.

A less rigid design allows full use of the advantages of porous ceramics and obtain a significantly higher output potential, as seen in Fig. 9(a). For a more rigid isotropic matrix, this effect is not observed. The EMCC decreases in both cases, while for a stiffer matrix after 50% porosity, the EMCC, as seen in Fig. 9(b), begins to decrease much faster, since the stiffness of the matrix in this case coincides with the rigidity of a rod with 50% pores. Bars with less rigidity cannot fully realize their electromechanical properties in such a configuration.

4. Conclusion

The paper considered two-level modeling of piezo-active composites using porous ceramics as an active material. The studied composite had a connectivity of 1-3 and consists of piezoceramic porous rods and an isotropic elastic matrix. The properties of porous ceramics and 1-3 composites were found by averaging in the ACELAN-COMPOS package based on various 3-0 and 1-3 models of representative volume elements. The effective properties of the final 1-3 composite were calculated for the two matrix materials. The stiffness of these matrices corresponded to the longitudinal stiffness of piezoceramic materials with a porosity of 50 % and 80 %. In some cases, formulas known from the literature can be used to determine the individual material constants of 1-3 composites. Using the finite element method, comparative numerical experiments were carried out for a complete model of several bodies and a model of one material with averaged properties. The adequacy of the second modeling step was verified by comparing the results for one fragment of a representative volume, considering the structure of materials and using effective properties. Eigenfrequencies and electromechanical coupling coefficient for different sets of material properties are determined. It was found that in the problem of forced vibrations, the output electric potential increases with growth of porosity. A certain feature was found in the case when the rigidity of the ceramic and the matrix coincide. In general, it can be noted that a 1-3 piezocomposite made of porous piezoceramics shows good properties as a green energy piezoelectric generator at high porosity and with a soft elastic matrix.

Author Contributions

A. Soloviev and A. Nasedkin defined the problems statement and methodology, A. Soloviev, A. Nasedkin and P. Oganesyan implemented discussed methods in ACELAN-COMPOS, D. Than Bin and P. Oganesyan developed finite element models and performed numerical experiments. The manuscript was written through the contribution of all authors. All authors discussed the results, reviewed, and approved the final version of the manuscript.

Acknowledgments

Conflict of Interest

The authors declared no potential conflicts of interest concerning the research, authorship, and publication of this article.

Funding

Data Availability Statements

The datasets generated and/or analyzed during the current study are available from the corresponding author on reasonable request.

Nomenclature

σ_{ij}	Components of stress tensor [N/m^2]	u_i	Components of displacement [m]
ε_{kl}	Components of strain tensor	φ	Electric potential [V]
D_i	Components of electric induction [C·m^{-2}]	ρ	Density [Kg/m^3]
E_k	Components of electric field vector [V/m]	$\mathbf{c}^E$	Tensor of elastic stiffness moduli
$\mathbf{e}$	Tensor of piezoelectric moduli	$\mathbf{k}^S$	Tensor of dielectric permittivities
k_{dj}	Electromechanical coupling coefficient		

References

[1] Ghazanfarian, J., Mohammadi, M.M., Uchino K., Piezoelectric energy harvesting: A systematic review of reviews, *Actuators*, 10(12), 2021, 312. https://doi.org/10.3390/act10120312

[2] Aabid, A., Raheman, M.A., Ibrahim, Y.E., Anjum, A., Hrairi, M., Parveez, B., Parveen, N., Mohammed Zayan, J., A systematic review of piezoelectric materials and energy harvesters for industrial applications, *Sensors*, 21, 2021, 4145. http://doi.org/10.3390/s21124145

[3] Banerjee, S., Bairagi, S., Wazed Ali, S., A critical review on lead-free hybrid materials for next generation piezoelectric energy harvesting and conversion, *Ceramics International*, 47, 2021, 16402–16421. http://doi.org/10.1016/j.ceramint.2021.03.054

[4] Li, T., Lee, P.S., Piezoelectric energy harvesting technology: From materials, structures, to applications, *Small Structures*, 3, 2022, 2100128. https://doi.org/10.1002/sstr.202100128

[5] Liu, Y., Khanbareh, H., Halim, M.A., Feeney, A., Zhang, X., Heidari, H., Ghannam, R., Piezoelectric energy harvesting for self-powered wearable upper limb applications, *Nano Select*, 2, 2021, 1459-1479. http://doi.org/10.1002/nano.202000242

[6] Mahapatra, S.D., Mohapatra, P.C., Aria, A.I., Christie, G., Mishra, Y.K., Hofmann, S., Thakur, V.K., Piezoelectric materials for energy harvesting and sensing applications: Roadmap for future smart materials, *Advanced Science*, 8, 2021, 2100864. https://doi.org/10.1002/advs.202100864

[7] Parinov, I.A., Cherpakov, A.V., Overview: State-of-the-Art in the energy harvesting based on piezoelectric devices for last decade, *Symmetry*, 14, 2022, 765. https://doi.org/10.3390/sym14040765

[8] Sezer, N., Koç, M., A comprehensive review on the state-of-the-art of piezoelectric energy harvesting, *Nano Energy*, 80, 2021, 105567, http://doi.org/10.1016/j.nanoen.2020.105567

[9] Chorsi, M.T., Curry, E.J., Chorsi, H.T., Das, R., Baroody, J., Purohit, P.K., Ilies, H., Nguyen, T.D., Piezoelectric biomaterials for sensors and actuators, *Advanced Materials*, 31, 2019, 1802084. https://doi.org/10.1002/adma.201802084

[10] Wang, Y., Hong, M., Venezuela, J., Liu, T., Dargusch, M., Expedient secondary functions of flexible piezoelectrics for biomedical energy harvesting, *Bioactive Materials*, 22, 2023, 291-311. https://doi.org/10.1016/j.bioactmat.2022.10.003

[11] Newnham, R.E., Skinner, D.P., Cross L.E., Connectivity and piezoelectric-pyroelectric composites, *Materials Research Bulletin*, 13(5), 1978, 525-536. https://doi.org/10.1016/0025-5408(78)90161-7

[12] Avellaneda, M., Swart, P.J., Calculating the performance of 1–3 piezocomposite for hydrophone applications: An effective medium approach, *Journal of the Acoustical Society of America*, 103, 1998, 1449–1467. http://doi.org/10.1121/1.421306

[13] Berger, H., Kari, S., Gabbert, U., Rodriguez-Ramos, R., Guinovart-Diaz, R., Otero, J.A., Bravo-Castillero, J., An analytical and numerical approach for calculating effective material coefficients of piezoelectric fiber composites, *International Journal of Solids and Structures*, 42, 2005, 5692–5714. http://doi.org/10.1016/j.ijsolstr.2005.03.016

[14] Bravo-Castillero, J., Guinovart-Diaz, R., Sabina, F.J., Rodríguez-Ramos, R., Closed-form expressions for the effective coefficients of a fiber-reinforced composite with transversely isotropic constituents – II. Piezoelectric and square symmetry, *Mechanics of Materials*, 33, 2001, 237–248. http://doi.org/10.1016/S0167-6636(00)00060-0

[15] Castillero, J.B., Diaz, R.G., Hernandez, J.A.O., Ramos R.R., Electromechanical properties of continuous fibre-reinforced piezoelectric composites, *Mechanics of Composite Materials*, 33, 1997, 475-482. https://doi.org/10.1007/BF02256903

[16] Gibiansky L.V., Torquato S., On the use of homogenization theory to design optimal piezocomposites for hydrophone applications, *Journal of the Mechanics and Physics of Solids*, 45(5), 1997, 689-708. https://doi.org/10.1016/S0022-5096(96)00106-8

[17] Guinovart-Dıaz, R., Bravo-Castillero, J., Rodrıguez-Ramos, R., Sabina, F.J., Martınez-Rosado, R., Overall properties of piezocomposite materials 1–3, *Materials Letters*, 48, 2001, 93–98. http://doi.org/10.1016/S0167-577X(00)00285-8

[18] Levin, V.M., Sabina, F.J., Bravo-Castillero, J., Guinovart-Díaz, R., Rodríguez-Ramos, R., Valdiviezo-Mijangos, O.C., Analysis of effective properties of electroelastic composites using the self-consistent and asymptotic homogenization methods, *International Journal of Engineering Science*, 46, 2008, 818–834. http://doi.org/10.1016/j.ijengsci.2008.01.017

[19] Sevostianov, I., Levin, V., Kachanov, M., On the modeling and design of piezocomposites with prescribed properties, *Archive of Applied Mechanics*, 71, 2001, 733–747. http://doi.org/10.1007/s004190100181

[20] Pramanik R., Arockiarajan A., Effective properties and nonlinearities in 1-3 piezocomposites: a comprehensive review, *Smart Materials and Structures*, 2019, 28, 103001. https://doi.org/10.1088/1361-665X/ab350a

[21] Aloui, R., Larbi, W., Chouchane, M., Uncertainty quantification and global sensitivity analysis of piezoelectric energy harvesting using macro fiber composites, *Smart Materials and Structures*, 29, 2020, 095014. http://doi.org/10.1088/1361-665X/ab9f12

[22] Shi, Y., Hallett, S.R., Zhu, M., Energy harvesting behaviour for aircraft composites structures using macro-fibre composite: Part I – Integration and experiment, *Composite Structures*, 160, 2017, 1279-1286. https://doi.org/10.1016/j.compstruct.2016.11.037.

[23] Song, H.J., Choi, Y.-T., Wereley, N.M., Purekar, A., Comparison of monolithic and composite piezoelectric material–based energy harvesting devices, *Journal of Intelligent Material Systems and Structures*, 25(14), 2014, 1825-1837. http://doi.org/10.1177/1045389X14530592

[24] Swallow, L.M., Luo, J.K., Siores, E., Patel, I., Dodds, D., A piezoelectric fibre composite based energy harvesting device for potential wearable applications, *Smart Materials and Structures*, 17, 2008, 025017. http://doi.org/10.1088/0964-1726/17/2/025017

[25] Della, C.N., Shu, D. Performance of 1–3 piezoelectric composites with porous piezoelectric matrix, *Applied Physics Letters*, 103, 2013, 132905. https://doi.org/10.1063/1.4822109

[26] Della, C.N., Shu, D.W., Della, C.N., Shu, D., The performance of 1–3 piezoelectric composites with a porous non-piezoelectric matrix, *Acta Materialia*, 56(4), 2008, 754-761. https://doi.org/10.1016/j.actamat.2007.10.022

[27] Gibiansky L.V., Torquato S., On the use of homogenization theory to design optimal piezocomposites for hydrophone applications, *Journal of the Mechanics and Physics of Solids*, 45(5), 1997, 689-708. https://doi.org/10.1016/S0022-5096(96)00106-8

[28] Sigmund, O., Torquato, S., Aksay, I.A. On the design of 1–3 piezocomposites using topology optimization, *Journal of Materials Research*, 13, 1998, 1038–1048. https://doi.org/10.1557/JMR.1998.0145

[29] Sladek J., Novak P., Bishay P.L., Sladek V., Effective properties of cement-based porous piezoelectric ceramic composites, *Construction and Building Materials*, 190, 2018, 1208-1214. https://doi.org/10.1016/j.conbuildmat.2018.09.127

[30] Nasedkin, A.V., Oganesyan, P.A., Soloviev, A.N., Analysis of Rosen type energy harvesting devices from porous piezoceramics with great longitudinal piezomodulus, *Zeitschrift für Angewandte Mathematik und Mechanik*, 101, 2021, e202000129. http://doi.org/10.1002/zamm.202000129

[31] Roscow, J.I., Lewis, R.W.C., Taylor, J., Bowen, C.R. Modelling and fabrication of porous sandwich layer barium titanate with improved piezoelectric energy harvesting figures of merit, *Acta Materialia*, 128, 2017, 207-217. http://dx.doi.org/10.1016/j.actamat.2017.02.029

[32] Rybyanets, A.N., Naumenko, A.A., Lugovaya, M.A., Shvetsova, N.A., Electric power generations from PZT composite and porous ceramics for energy harvesting devices, *Ferroelectrics*, 484, 2015, 95-100. https://doi.org/10.1080/00150193.2015.1060065

[33] Yan, M., Xiao, Z., Ye, J., Yuan, X., Li, Z., Bowen, C., Zhang, Y., Zhang, D., Porous ferroelectric materials for energy technologies: current status and future perspectives, *Energy & Environmental Science*, 14(12), 2021, 6158-6190. http://doi.org/10.1039/d1ee03025f

[34] Gerasimenko, T.E., Kurbatova, N.V., Nadolin, D.K., Nasedkin, A.V., Nasedkina, A.A., Oganesyan, P.A., Skaliukh, A.S., Soloviev, A.N., Homogenization of piezoelectric composites with internal structure and inhomogeneous polarization in ACELAN-COMPOS finite element package. In: Sumbatyan, M.A., (ed) *Wave Dynamics, Mechanics and Physics of Microstructured Metamaterials*. Advanced Structured Materials, 109, Springer: Singapore, 2019, 113–131. http://doi.org/10.1007/978-3-030-17470-5_8

[35] Kurbatova, N.V., Nadolin, D.K., Nasedkin, A.V., Oganesyan, P.A., Soloviev A.N., Finite element approach for composite magneto-piezoelectric materials modelling in ACELAN-COMPOS Package. In: Altenbach, H., Carrera, E., Kulikov, G., (eds) *Analysis and Modelling of Advanced Structures and Smart Systems*. Advanced Structured Materials, 81, Singapore: Singapore, 2018, 69-88. http://doi.org/10.1007/978-981-10-6895-9_5

[36] Belokon', A.V., Nasedkin, A.V., Solov'ev, A.N., New schemes for the finite-element dynamic analysis of piezoelectric devices, *Journal of Applied Mathematics and Mechanics*, 66, 2002, 481–490. http://doi.org/10.1016/S0021-8928(02)00058-8

[37] Nasedkin, A.V., Some finite element methods and algorithms for solving acousto-piezoelectric problems. In: Parinov, I.A., (ed) *Piezoceramic Materials and Devices*, Nova Science Publishers, New York, 2010, 177–218.

[38] Dunn, M.L., Taya, M., Micromechanics predictions of the effective electroelastic moduli of piezoelectric composites, *International Journal of Solids and Structures*, 30, 1993, 161–175. http://doi.org/10.1016/0020-7683(93)90058-F

[39] Hori, M., Nemat-Nasser, S., Universal bounds for effective piezoelectric moduli, *Mechanics of Materials*, 30, 1998, 295-308. doi: 10.1016/S0167-6636(98)00029-5

[40] Kar-Gupta, R., Venkatesh, T.A., Electromechanical response of porous piezoelectric materials, *Acta Materialia*, 54, 2006, 4063–4078. http://doi.org/10.1016/j.actamat.2006.04.037

[41] Martínez-Ayuso, G., Friswell, M.I., Adhikari, S., Khodaparast, H.H., Berger, H., Homogenization of porous piezoelectric materials, *International Journal of Solids and Structures*, 113–114, 2017, 218–229. http://doi.org/10.1016/j.ijsolstr.2017.03.003

[42] Mawassy, N., Reda, H., Ganghoffer, J.-F., Eremeyev, V.A., Lakiss, H., A variational approach of homogenization of piezoelectric composites towards piezoelectric and flexoelectric effective media, *International Journal of Engineering Science*, 158, 2021, 103410. https://doi.org/10.1016/j.ijengsci.2020.103410

[43] Nasedkin, A.V., Shevtsova, M.S., Improved finite element approaches for modelling of porous piezocomposite materials with different connectivity. In: Parinov, I.A., (ed) *Ferroelectrics and Superconductors: Properties and Applications*, Nova Science Publishers, New York, 2011, 231–254.

[44] Nasedkin, A.V., Nasedkina, A.A., Nassar, M.E., Homogenization of porous piezocomposites with extreme properties at pore boundaries by effective moduli method, *Mechanics of Solids*, 55(6), 2020, 827–836. https://doi.org/10.3103/S0025654420050131

[45] Odegard, G.M., Constitutive modeling of piezoelectric polymer composites, *Acta Materialia*, 52, 2004, 5315–5330, https://doi.org/10.1016/j.actamat.2004.07.037

[46] Nasedkin, A., Nassar, M.E., About anomalous properties of porous piezoceramic materials with metalized or rigid surfaces of pores, *Mechanics of Materials*, 162, 2021, 104040. http://doi.org/10.1016/j.mechmat.2021.104040

[47] Firooz, S., Steinmann, P., and Javili, A., Homogenization of composites with extended general interfaces: Comprehensive review and unified modeling, *Applied Mechanics Reviews*, 73(4), 2021, 040802. https://doi.org/10.1115/1.4051481

[48] Kudimova, A.B., Nadolin, D.K., Nasedkin, A.V., Oganesyan, P.A., Soloviev, A.N., Finite element homogenization models of bulk mixed piezocomposites with granular elastic inclusions in ACELAN package, *Materials Physics and Mechanics*, 37, 2018, 25–33. http://doi.org/10.18720/MPM.3712018_4

[49] Kudimova, A.B., Nadolin, D.K., Nasedkin, A.V., Nasedkina, A.A., Oganesyan, P.A. Soloviev, A.N., Finite element homogenization of piezocomposites with isolated inclusions using improved 3-0 algorithm for generating representative volumes in ACELAN-COMPOS package, *Materials Physics and Mechanics*, 44, 2020, 392-403. http://doi.org/ 10.18720/MPM.4432020_10

[50] El Moumen, A., Kanit, T., Imad, A., Numerical evaluation of the representative volume element for random composites, *European Journal of Mechanics/A Solids*, 86, 2021, 104181. https://doi.org/10.1016/j.euromechsol.2020.104181

[51] Kari, S., Berger, H., Rodriguez-Ramos, R., Gabbert, U., Computational evaluation of effective material properties of composites reinforced by randomly distributed spherical particles, *Composite Structures*, 77, 2007, 223–231. http://doi.org/10.1016/j.compstruct.2005.07.003

[52] Segurado, J., Llorca, J., A numerical approximation to the elastic properties of sphere reinforced composites, *Journal of the Mechanics and Physics of Solids*, 50, 2002, 2107–2121. http://doi.org/10.1016/S0022-5096(02)00021-2

[53] Schröder, J., Balzani, D., Brands, D., Approximation of random microstructures by periodic statistically similar representative volume elements based on lineal-path functions, *Archive of Applied Mechanics*, 81, 2011, 975–997. http://doi.org/10.1007/s00419-010-0462-3

[54] COMSOL Multiphysics® v. 5.6. www.comsol.com. COMSOL AB, Stockholm, Sweden. (License № 9602094)

ORCID iD

Andrey Nasedkin https://orcid.org/0000-0002-3883-2799
Pavel Oganesyan https://orcid.org/0000-0003-2311-7562
Arcady Soloviev https://orcid.org/0000-0001-8465-5554

How to cite this article: Do T.B., Nasedkin A., Oganesyan P., Soloviev A. Multilevel Modeling of 1-3 Piezoelectric Energy Harvester Based on Porous Piezoceramics, *J. Appl. Comput. Mech.*, 9(3), 2023, 763–774. https://doi.org/10.22055/jacm.2023.42264.3900

Publisher's Note Shahid Chamran University of Ahvaz remains neutral with regard to jurisdictional claims in published maps and institutional affiliations.